

Cerebellar Volume and Disease Staging in Parkinson's Disease: An ENIGMA-PD Study

Rebecca Kerestes, PhD,^{1*}  Max A. Laansma, MSc,^{2,3}  Conor Owens-Walton, PhD,⁴ Andrew Perry, PhD,⁵ Eva M. van Heese, BSc,^{2,3} Sarah Al-Bachari, PhD, MBChB,⁶ Tim J. Anderson, FRACP, MD,^{7,8} Francesca Assogna, PhD,⁹ Ítalo K. Aventura, MD,^{10,11} Tim D. van Balkom, PhD,^{2,3,12}  Henk W. Berendse, MD, PhD,¹³ Kevin R.E. van den Berg, MD,^{14,15} Rebecca Betts, Mphys,¹⁶ Ricardo Brioschi, MD,¹⁰ Jonathan Carr, MBChB, PhD,¹⁷ Fernando Cendes, MD, PhD,^{10,11}  Lyles R. Clark, PhD,¹⁸ John C. Dalrymple-Alford, PhD,^{7,19,20} Michiel F. Dirks, MD, PhD,²¹ Jason Druzgal, MD, PhD,²² Helena Durrant, Mphys,¹⁶ Hedley C.A. Emsley, PhD, FRCP,^{23,24} Gaëtan Garraux, PhD,^{25,26} Hamied A. Haroon, PhD,²⁷ Rick C. Helmich, MD, PhD,^{14,15}  Odile A. van den Heuvel, MD, PhD,^{2,3,12} Rafael B. João, MD, MSc,^{10,11} Martin E. Johansson, MSc,²¹ Samson G. Khachatryan, MD, PhD,^{28,29} Christine Lochner, PhD,³⁰ Corey T. McMillan, PhD,¹⁸ Tracy R. Melzer, PhD,^{7,19,20}  Philip E. Mosley, MD, PhD,^{31,32} Benjamin Newman, PhD,²² Peter Opiessnig, PhD,³³ Laura M. Parkes, PhD,^{34,35}  Clelia Pellicano, MD, PhD,⁹ Fabrizio Piras, PhD,⁹ Toni L. Pitcher, PhD,^{7,19}  Kathleen L. Poston, MD, PhD,³⁶  Mario Rango, MD, PhD,^{37,38} Annerine Roos, PhD,³⁹ Christian Rummel, PhD,⁴⁰ Reinhold Schmidt, MD, PhD,⁴¹ Petra Schwingsenschuh, MD,⁴¹ Lucas S. Silva, MD, MSc,^{10,11} Viktorija Smith, MSc,³⁶ Letizia Squarcina, PhD,⁴² Dan J. Stein, MD,³⁹ Zaruhi Tavadyan, MD,^{28,29} Chih-Chien Tsai, PhD,⁴³ Daniela Vecchio, PhD,⁹ Chris Vriend, PhD,^{2,12,44} Jiun-Jie Wang, PhD,^{43,45,46,47}  Roland Wiest, MD, PhD,⁴⁰ Clarissa L. Yasuda, MD, PhD,^{10,11} Christina B. Young, PhD,³⁶ Neda Jahanshad, PhD,⁴ Paul M. Thompson, PhD,⁴ Ysbrand D. van der Werf, PhD,^{2,3} Ian H. Harding, PhD,^{1,48}  and the ENIGMA-Parkinson's Study

¹Department of Neuroscience, Central Clinical School, Monash University, Melbourne, Victoria, Australia

²Department Anatomy and Neurosciences, Amsterdam UMC, Vrije Universiteit Amsterdam, Amsterdam, The Netherlands

³Amsterdam Neuroscience, Neurodegeneration, Amsterdam, The Netherlands

⁴Imaging Genetics Center, Mark and Mary Stevens Neuroimaging and Informatics Institute, Keck School of Medicine, University of Southern California, Marina del Rey, California, USA

⁵Monash Bioinformatics Platform, Monash University, Melbourne, Victoria, Australia

⁶Faculty of Health and Medicine, The University of Lancaster, Lancaster, United Kingdom

⁷New Zealand Brain Research Institute, Christchurch, New Zealand

⁸Neurology Department, Te Whatu Ora - Health New Zealand Waitaha Canterbury, Christchurch, New Zealand

⁹Laboratory of Neuropsychiatry, IRCCS Santa Lucia Foundation, Rome, Italy

¹⁰Department of Neurology, University of Campinas – UNICAMP, Campinas, Brazil

¹¹Brazilian Institute of Neuroscience and Neurotechnology, Campinas, Brazil

¹²Department Psychiatry, Amsterdam UMC, Vrije Universiteit Amsterdam, Amsterdam, The Netherlands

¹³Department Neurology, Amsterdam UMC, Vrije Universiteit Amsterdam, Amsterdam, The Netherlands

¹⁴Department of Neurology and Center of Expertise for Parkinson and Movement Disorders, Donders Institute for Brain, Cognition and Behaviour, Radboud University Medical Centre, Nijmegen, The Netherlands

¹⁵Centre for Cognitive Neuroimaging, Donders Institute for Brain, Cognition and Behaviour, Radboud University Nijmegen, Nijmegen, The Netherlands

This is an open access article under the terms of the [Creative Commons Attribution-NonCommercial-NoDerivs](https://creativecommons.org/licenses/by-nc-nd/4.0/) License, which permits use and distribution in any medium, provided the original work is properly cited, the use is non-commercial and no modifications or adaptations are made.

***Correspondence to:** Rebecca Kerestes, Department of Neuroscience, Monash University, Level 6, The Alfred Center, 99 Commercial Road, Prahran, VIC 3004, Australia; E-mail: rebecca.kerestes@monash.edu

Relevant conflicts of interest/financial disclosures: P.S. reports personal fees from Bial, AbbVie and Boston Scientific. G.G. owns stocks in Koios Care (<https://www.koios.care/>) and has received consultancy fees from AbbVie Belgium, Zambon Belgium, and EG Belgium (Stada group). He also received an honorarium from AbbVie Belgium, Zambon Belgium, and EG Belgium. M.D. has received honoraria from Movement Disorders Society, Quebec. I.H.H. has provided consulting services to PTC Therapeutics, Steminent Biotherapeutics, BioAge Labs, Excure Inc, unrelated to this work. K.P. owns stocks in Amprion and Curasen. She has also received honoraria from invited scientific presentations to universities and professional societies not exceeding \$5000/year and provides consulting services to Curasen. D.J.S. has received

consultancy fees from Discovery Vitality, Johnson and Johnson, Kanna, L'Oreal, Lundbeck, Orion, Sanofi, Servier, Takeda, and Vistagen. He has also received royalties from American Psychiatric Publishing, Cambridge University Press, Elsevier Press, and Oxford University Press.

Funding agencies: ENIGMA Core—This work was supported in part by National Institutes of Health (NIH) grants R01NS107513, R01AG058854, R01AG059874, R01MH116147, R01MH117601, and U54EB020403, The Michael J. Fox Foundation grant 14848. Parkinson's Progression Markers Initiative (PPMI), data used in the preparation of this article were obtained from PPMI database (www.ppmi-info.org/access-data-specimens/download-data). For up-to-date information on the study, visit www.ppmi-info.org. PPMI, a public-private partnership, is funded by The Michael J. Fox Foundation for Parkinson's Research and funding partners, including 4D Pharma, AbbVie, AcureX Therapeutics, Allergan, Amathus Therapeutics, Aligning Science Across Parkinson's (ASAP), Avid Radiopharmaceuticals, Bial Biotech, Biogen, BioLegend, Bristol-Myers Squibb, Celgene Corporation, DaCapo Brainscience, Denali Therapeutics, The Edmond J. Safra Foundation, Eli Lilly and Company, GE Healthcare, GlaxoSmithKline, Golub Capital, Handi Therapeutics, Insite, Janssen Pharmaceuticals, Lundbeck, Merck and Co Inc, Meso Scale Diagnostics (MSD), LLC, Neurocrine Biosciences, Pfizer Inc,

¹⁶*School of Physics and Astronomy, Faculty of Science and Engineering, The University of Manchester, Manchester, United Kingdom*

¹⁷*Division of Neurology, Tygerberg Hospital and Stellenbosch University, Cape Town, South Africa*

¹⁸*Department of Neurology, University of Pennsylvania Perelman School of Medicine, Philadelphia, Pennsylvania, USA*

¹⁹*Department of Medicine, University of Otago, Christchurch, New Zealand*

²⁰*School of Psychology, Speech and Hearing, University of Canterbury, Christchurch, New Zealand*

²¹*Department of Neurology and Center of Expertise for Parkinson and Movement Disorders, Donders Institute for Brain, Cognition and Behaviour, Radboud University Nijmegen Medical Centre, Nijmegen, The Netherlands*

²²*Department of Radiology and Medical Imaging, University of Virginia, Charlottesville, Virginia, USA*

²³*Lancaster Medical School, Lancaster University, Lancaster, United Kingdom*

²⁴*Division of Neuroscience and Experimental Psychology, Faculty of Biology, Medicine and Health, The University of Manchester, Manchester Academic Health Science Centre, Manchester, United Kingdom*

²⁵*GIGA-CRC in vivo imaging, University of Liège, Liège, Belgium*

²⁶*MoVeRe group, Department of Neurology, CHU de Liège, Belgium*

²⁷*Division of Psychology, Communication and Human Neuroscience, Faculty of Biology, Medicine and Health, The University of Manchester, Manchester Academic Health Science Centre, Manchester, United Kingdom*

²⁸*Department of Neurology and Neurosurgery, National Institute of Health, Yerevan, Armenia*

²⁹*Centers for Sleep and Movement Disorders, Somnus Neurology Clinic, Yerevan, Armenia*

³⁰*Department of Psychiatry, SA MRC Unit on Risk and Resilience in Mental Disorders, Stellenbosch University, Cape Town, South Africa*

³¹*Clinical Brain Networks Group, QIMR Berghofer Medical Research Institute, Brisbane, Queensland, Australia*

³²*The Australian eHealth Research Centre, CSIRO Health and Biosecurity, Brisbane, Queensland, Australia*

³³*Department of Neurology, Clinical Division of Neurogeriatrics, Medical University Graz, Graz, Austria*

³⁴*Division of Psychology, Communication and Human Neuroscience, School of Health Sciences, Faculty of Biology, Medicine and Health, The University of Manchester, Manchester, United Kingdom*

³⁵*Geoffrey Jefferson Brain Research Centre, Manchester Academic Health Science Centre, Northern Care Alliance and University of Manchester, Manchester, United Kingdom*

³⁶*Department of Neurology and Neurological Sciences, Stanford University, Palo Alto, California, USA*

³⁷*Excellence Center for Advanced MR Techniques and Parkinson's Disease Center, Neurology unit, Fondazione IRCCS Cà Granda Maggiore Policlinico Hospital, University of Milan, Milan, Italy*

³⁸*Department of Neurosciences, Neurology Unit, Fondazione Ca' Granda, IRCCS, Ospedale Policlinico, University of Milan, Milano, Italy*

³⁹*Department of Psychiatry and Neuroscience Institute, SA MRC Unit on Risk and Resilience in Mental Disorders, University of Cape Town, Cape Town, South Africa*

Piramal Imaging, Prevail Therapeutics, F. Hoffmann-La Roche Ltd and its affiliated company Genentech Inc, Sanofi Genzyme, Servier, Takeda Pharmaceutical Company, Teva Neuroscience Inc, UCB, Vanqua Bio, Verily Life Sciences, Voyager Therapeutics Inc, and Yumanity Therapeutics Inc. OpenNeuro Japan cohort—These data were obtained from the OpenfMRI database. Its accession number is ds000245. This research was supported in part by the following: a Grant-in-Aid from the Research Committee of Central Nervous System Degenerative Diseases by the Ministry of Health, Labour, and Welfare, Integrated Research on Neuropsychiatric Disorders project, carried out by SRBPS; a Grant-in-Aid for Scientific Research on Innovative Areas (Brain Protein Aging and Dementia Control 26,117,002) from the MEXT of Japan; Integrated Research on Neuropsychiatric Disorders carried out under the Strategic Research Program for Brain Sciences, Scientific Research on Innovative Areas (Comprehensive Brain Science Network); and Integrated Research on Depression, Dementia, and Development Disorders by the Strategic Research Program for Brain Sciences from the Japan Agency for Medical Research and Development (AMED). NEUROCON cohort—This work was partially supported by the NEUROCON project (84/2012), financed by UEFISCDI. Brisbane cohorts—This work was funded by a Royal Brisbane and Women's Hospital Foundation Project Grant, an Early-Career Investigator Grant from the Royal Australian and New Zealand College of Psychiatrists and an Advance Queensland Early Career Investigator Grant. Stanford cohort—This work was supported by the NIH/The National Institute of Neurological Disorders and Stroke (NINDS) (R01 NS115114; R01 NS107513) (K23 NS075097) and The Michael J. Fox Foundation for Parkinson's Research. Amsterdam I cohort—Grant support (6440) from the Netherlands Organization for Health Research and Development, The Michael J. Fox Foundation, and the Hersenstichting. Amsterdam II (Cogtips) cohort—Cogtips is supported by the Dutch Parkinson's Disease Association ("Parkinson Vereniging" 2015-R04) and Brain Foundation of the Netherlands ("Hersenstichting" HA-2017-00227). Liege I and II cohorts—This work was funded by PDR Grant T0.165.14, National Fund for Scientific Research (FNRS), Belgium. Donders I cohort—This work was funded by a grant of the Dutch Brain Foundation (grant F2013[10-15]), from the Netherlands Organization for Scientific Research (VENI grant 91617077, VIDI grant 09150172010044), and from The Michael J. Fox Foundation. Donders II cohort—This work was funded by Verily Life Sciences, Health-Holland, The Michael J. Fox Foundation for Parkinson's

Research (grant ID 15581), The city of Nijmegen, The province of Gelderland and a center of excellence grant from the Parkinson's Foundation. Rome SLF cohort—This work was funded by the Italian Ministry of Health, RC12-13-14-15-16-17-18-19/A. UNICAMP cohort—This work was funded by the São Paulo Research Foundation (FAPESP 2023/11469-1; 2013-07559-3). Christchurch cohort—This work was supported by the Health Research Council of New Zealand (14-440, 14-573), Canterbury Medical Research Foundation (12/01), and Neurological Foundation of New Zealand (1635-PG), University of Otago Research Grant, Brain Research New Zealand. Charlottesville I-III cohorts—This work was supported by grants from the Department of Defense, Commonwealth of Virginia's Alzheimer's and Related Diseases Research Award Fund, and University of Virginia. Manchester I and II cohorts—This work was funded by the Sydney Driscoll Neuroscience Foundation, Lancaster University, and the Sir John Fisher Foundation (LP), University of Manchester Biomedical Imaging Institute, Medical Research Council United Kingdom (UK) Doctoral Training Program (SA), Engineering and Physical Science Research Council UK (EP/M005909/1). Pennsylvania cohort—This work was funded by the NINDS, NIH AG062418 (U19), and NS053488 (P50). Chang Gung cohort—This work was supported by National Science and Technology Council (NSTC 109-2221-E-182-009-MY3, NSTC 109-2314-B-182-021-MY3, NSTC 112-2314-B-182-052-MY3); the Healthy Aging Research Center (grant EMRPD1M0451, EMRPD1M0431); and the Chang Gung Memorial Hospital (CMRPD1L0141). UDALL—This work was funded by NIH grants RC4 NS073008 and P50 NS062684, and Ruth L. Kirschstein National Research Service Award T32AG0000258. Data paper: <https://doi.org/10.1089/brain.2014.0248>. Bern cohorts—This work was funded by the Swiss National Science Foundation (SNF, project 204593, "ScanOMetrics"). Stanford I and II cohorts—Funded by NIH/NINDS NS075097, NS115114, and The Michael J. Fox Foundation.

Rebecca Kerestes and Max A. Laansma contributed equally to this paper.

Received: 29 May 2023; **Revised:** 14 August 2023; **Accepted:** 11 September 2023

Published online 14 November 2023 in Wiley Online Library
([wileyonlinelibrary.com](https://www.wileyonlinelibrary.com)). DOI: 10.1002/mds.29611

⁴⁰Support Center for Advanced Neuroimaging, (SCAN) University Institute of Diagnostic and Interventional Neuroradiology, Inselspital, Bern University Hospital, University of Bern, Bern, Switzerland

⁴¹Department of Neurology, Medical University of Graz, Graz, Austria

⁴²Department of Pathophysiology and Transplantation, University of Milan, Milan, Italy

⁴³Healthy Aging Research Center, Chang Gung University, Taoyuan City, Taiwan

⁴⁴Amsterdam Neuroscience, Brain Imaging, Amsterdam, The Netherlands

⁴⁵Department of Medical Imaging and Radiological Sciences, Chang Gung University, Taoyuan City, Taiwan

⁴⁶Department of Diagnostic Radiology, Chang Gung Memorial Hospital Keelung Branch, Keelung City, Keelung, Taiwan

⁴⁷Department of Chemical Engineering, Ming-Chi University of Technology, New Taipei City, Taiwan

⁴⁸Monash Biomedical Imaging, Monash University, Melbourne, Victoria, Australia

ABSTRACT: Background: Increasing evidence points to a pathophysiological role for the cerebellum in Parkinson's disease (PD). However, regional cerebellar changes associated with motor and non-motor functioning remain to be elucidated.

Objective: To quantify cross-sectional regional cerebellar lobule volumes using three dimensional T1-weighted anatomical brain magnetic resonance imaging from the global ENIGMA-PD working group.

Methods: Cerebellar parcellation was performed using a deep learning-based approach from 2487 people with PD and 1212 age and sex-matched controls across 22 sites. Linear mixed effects models compared total and regional cerebellar volume in people with PD at each Hoehn and Yahr (HY) disease stage, to an age- and sex-matched control group. Associations with motor symptom severity and Montreal Cognitive Assessment scores were investigated.

Results: Overall, people with PD had a regionally smaller posterior lobe ($d_{\max} = -0.15$). HY stage-specific

analyses revealed a larger anterior lobule V bilaterally ($d_{\max} = 0.28$) in people with PD in HY stage 1 compared to controls. In contrast, smaller bilateral lobule VII volume in the posterior lobe was observed in HY stages 3, 4, and 5 ($d_{\max} = -0.76$), which was incrementally lower with higher disease stage. Within PD, cognitively impaired individuals had lower total cerebellar volume compared to cognitively normal individuals ($d = -0.17$).

Conclusions: We provide evidence of a dissociation between anterior "motor" lobe and posterior "non-motor" lobe cerebellar regions in PD. Whereas less severe stages of the disease are associated with larger motor lobe regions, more severe stages of the disease are marked by smaller non-motor regions. © 2023 The Authors. *Movement Disorders* published by Wiley Periodicals LLC on behalf of International Parkinson and Movement Disorder Society.

Key Words: cerebellum; disease staging; MRI; Parkinson's disease

Introduction

Anatomical abnormalities at the cerebral cortical and subcortical level are diffuse in Parkinson's disease (PD), and have been reported across all symptomatic disease stages, in line with the progressive nature of PD.¹ Although the cerebellum is recognized for its cardinal role in motor functioning as well as various non-motor domains,^{2–9} relatively little research has been dedicated to characterizing the morphology of the cerebellum in PD.

Anatomically, the cerebellum consists of two hemispheres separated by the vermis, and is divided along its superior to inferior axis into three lobes: anterior, posterior, and flocculonodular. The lobes are further subdivided into 10 lobules, denoted by Roman numerals I–X.^{10,11} The anterior lobe, comprising lobules I–V, is largely associated with motor processes;^{12,13} the posterior lobe, comprising lobules VI–IX, can be further divided into superior (lobules VI, Crus I and II [ie, VIIA], and

VIIIB) and inferior (lobules VIIIA and VIIIB) divisions that represent non-motor and motor functional divisions, respectively.^{14,15} Last, the flocculonodular lobe, comprising lobule X, is implicated in the governing of eye movements and body equilibrium during stance and gait.¹¹

Perhaps surprisingly, a voxel-based morphometry meta-analysis from 2017 revealed no differences in cerebellar structure in people with PD compared to controls. This was possibly explained by heterogeneous clinical characteristics of the PD samples examined.¹⁶ Furthermore, there is evidence to suggest that hypertrophy of subcortical regions may occur in mild stages of PD, which would further nuance meta-analysis findings.¹ Other case-control findings suggest the involvement of the vermis, Crus I, and lobule VI in PD,^{17,18} partly supported by a longitudinal analysis demonstrating subregional cerebellar atrophy in lobules I–IV, VI, Crus I, Crus II, VIIIB, VIIIA, VIIIB, and the vermis.¹⁹ Some studies have shown associations between cerebellar atrophy and motor symptoms, cognitive

dysfunction, and disease severity.^{16,20–22} In a recent study, higher volume of lobule IV was associated with a higher intensity of resting tremor and total tremor severity in people with PD.²³ Although there is some evidence to suggest cerebellar involvement is restricted to tremor-predominant patients,¹⁸ findings have been inconsistent.¹⁶ More spatially precise examinations of regional cerebellar volume in larger, more diverse samples are required to understand the PD-related changes in cerebellar structure associated with disease staging and its association with motor severity and cognitive functioning.

The development of new machine learning based approaches for optimized and automated feature-based parcellation of the cerebellum allows for more spatially precise, finer-grained mapping of cerebellar anatomy.²⁴ One such approach, called automatic cerebellum anatomical parcellation using u-net with locally constrained optimization (ACAPULCO), uses a deep learning algorithm to automatically parcellate the cerebellum into 28 anatomical subunits.²⁵ ACAPULCO performs on par with leading approaches for automatic cerebellar parcellation including CERES2, has broad applicability to both healthy and atrophied cerebellums, and is more time-efficient than other approaches.²⁵

Here, we applied the standardized ENIGMA cerebellum parcellation protocol (<https://enigma.ini.usc.edu/protocols/imaging-protocols/>), which uses ACAPULCO to quantify cerebellar lobule volumes from 2847 adults with PD and 1212 controls from the global ENIGMA-PD working group.²⁶ We ran multi-site mega-analyses to infer regional cerebellar volumetric differences people with PD compared to controls, comparing Hoehn and Yahr (HY) stages 1, 2, 3, and 4–5 with age- and sex-matched control groups. Relationships between total and regional cerebellar volume and (1) time since diagnosis, and (2) motor symptom severity were assessed. Finally, exploratory analyses were conducted to assess cerebellar volume differences between PD with and without cognitive impairment.

Methods

Sample Characteristics

Twenty-two sites were included in this cross-sectional study, totaling 2487 adults with PD and 1212 controls (Tables 1 and 2). Clinical information from the PD subjects included HY stage, time since diagnosis, age of onset of PD, scores from the Movement Disorder Society (MDS) sponsored revision of the Unified Parkinson's Disease Rating Scale part 3 (UPDRS3) obtained in the ON or OFF state,²⁷ medication status (currently *on* or *off* medication) and Montreal

Cognitive Assessment (MoCA) score (Table 2).²⁸ Individual-site inclusion and exclusion criteria are provided in Supplementary Table S1. Some sites contributed multiple cohorts from separate testing environments including different magnetic resonance imaging (MRI) scanning acquisitions, yielding a total of 30 samples, henceforth referred to as “cohorts” (see “Image Processing and Analysis” section below). Disease severity was assessed using HY stages ranging from 1 to 5, from HY1, “unilateral involvement only usually with minimal or no functional disability,” to HY5, “confinement to bed or wheelchair unless aided.” The modified HY scale,²⁹ which includes intermediate increments of 1.5 and 2.5 to complement stage 2 was used in 13 cohorts. We regrouped the cases so that HY1.5 (n = 79) and HY2.5 (n = 208) individuals were included in the HY2 group. The HY4 (n = 67) and HY5 (n = 19) groups were merged into HY4–5, given their smaller samples. To address the issue of some people with PD being assessed with the original UPDRS and some being assessed with the MDS-UPDRS, we used a validated formula to convert original UPDRS3 scores to predicted MDS-UPDRS3 scores.³⁰

Image Processing and Analysis: ACAPULCO

Whole-brain, T1-weighted three-dimensional volumetric magnetic resonance images were collected from each participant. Scanner descriptions and acquisition protocols for all sites are reported in Supplementary Table S2. We treated each individual scanner and/or data acquisition protocol used in the collection of MRI scans as a separate cohort during statistical analysis (see below). Each image was processed in accordance with the ENIGMA cerebellum parcellation protocol, as fully described elsewhere (<https://enigma.ini.usc.edu/protocols/imaging-protocols/>).²⁶ In brief, the cerebellum was parcellated into 28 subregions (left and right lobules I–III, IV, V, VI, Crus I, Crus II, VIIB, VIIIA, VIIIB, IX, and X; bilateral vermis VI, VII, VIII, IX, and X, and bilateral corpus medullare (central white matter) using ACAPULCO (version 0.2.1; <https://gitlab.com/shuohan/acapulco>).²⁵ As part of the pipeline, a measure of intracranial volume (ICV) is calculated for each participant using Freesurfer. At the individual-level, parcellated cerebellar masks were quality checked for segmentation errors (ie, over or under inclusion of individual lobules) by visual inspection of the cerebellar mask overlaid on the respective participants T1 image. This was followed by quantitative identification of outlier volumes that were greater or less than 2.698 standard deviations from the group mean. Outlier volumes (treated as not available) were subsequently excluded from group-level statistical analyses.

TABLE 1 Demographic and clinical characteristics of the sample

Site	Cohort	Age controls		Age cases		Female (%)		Age of onset		Duration of illness		Total controls	Total cases	MDS-UPDRS
		Mean (SD)	Mean (SD)	Mean (SD)	Mean (SD)	Controls	Cases	Mean (SD)	Mean (SD)					
Amsterdam	Amsterdam I*	56.5 (9.6)	63.3 (10.6)	37	39	62.2 (11.2)	2.1 (2.4)	43	134	No				
	Amsterdam II	61.5 (9.5)	63.4 (7.1)	40	40	58.3 (7.9)	5.3 (3.8)	25	78	No				
Bern	Bern I	52.7 (9.5)	63.0 (10.6)	25	54	50.0 (10.4)	12.3 (4.2)	20	50	Yes				
	Bern II	67.6 (4.6)	60.2 (5.6)	67	50	47.0 (6.4)	13.7 (7.9)	36	4	No				
Brisbane	Brisbane I	-	60.9 (9.5)	-	24	NA	9.7 (6.1)	-	25	No				
	Brisbane II	-	62.3 (9.7)	-	33	54.1 (9.6)	8.2 (4.2)	-	58	No				
CapeTown	CapeTown	68.5 (6.3)	66.1 (5.6)	33	9	60.7 (5.9)	6.2 (3.8)	9	11	No				
Chang Gung	CGU*	61.0 (7.3)	59.9 (9.5)	42	43	51.8 (10.9)	8.6 (6.4)	227	322	No				
Charlottesville	Charlottesville I	-	63.7 (9.1)	-	24	54.1 (9.8)	9.6 (5.1)	-	92	Yes				
	Charlottesville II	-	62.0 (9.0)	-	13	53.4 (9.9)	8.6 (3.6)	-	30	Yes				
	Charlottesville III	-	71.3 (6.7)	-	32	63.4 (7.6)	8.0 (3.2)	-	22	Yes				
Christchurch	PDNZ	69.1 (8.2)	69.3 (7.7)	35	27	63.6 (8.6)	5.6 (5.5)	52	201	Yes				
Donders	Donders I**	62.7 (10.3)	61.2 (9.9)	48	44	58.1 (10.8)	4.4 (3.9)	23	57	Yes				
	Donders II*	59.6 (9.6)	61.5 (8.9)	50	45	58.8 (8.9)	2.6 (1.5)	54	432	Yes				
Graz	PROMOVE/ASPS I	63.4 (10.1)	63.2 (10.4)	28	28	58.5 (10.6)	4.7 (4.6)	120	97	Yes				
	PROMOVE/ASPS II	-	64.0 (9.9)	-	22	60.0 (11.1)	4.0 (3.7)	-	23	Yes				
Liege	Liege	64.7 (6.4)	65.6 (7.3)	49	44	58.8 (7.3)	6.8 (4.6)	63	61	No				
Manchester	Manchester	66.5 (6.9)	69.0 (7.8)	54	25	61.1 (9.6)	7.6 (4.9)	35	49	Yes				
Milan	Milan*	53.2 (8.3)	52.5 (6.9)	71	50	44.2 (7.8)	11.3 (6.4)	21	8	Not available				
Neurocon	Neurocon	67.7 (11.5)	68.7 (10.7)	86	38	NA	NA	14	26	Yes				
ON Japan	Openneuro	63.3 (5.2)	66.6 (6.7)	53	54	NA	NA	15	26	Not available				
PPMI	PPMI	60.3 (10.7)	61.4 (10.1)	45	40	60.8 (10.0)	0.5 (0.5)	109	228	Yes				
Rome SLF	Rome SLF	37.1 (10.8)	61.9 (10.5)	38	33	57.1 (11.2)	4.7 (4.4)	110	166	No				
Stanford	Stanford I	62.9 (10.2)	65.2 (9.7)	72	60	60.9 (9.5)	4.8 (3.3)	18	30	Yes				
	Stanford II	70.2 (4.9)	70.2 (8.0)	62	44	65.4 (7.8)	5.0 (3.5)	21	50	Yes				

(Continues)

TABLE 1 Continued

Site	Cohort	Age controls		Age cases		Female (%)		Age of onset		Duration of illness		Total controls	Total cases	MDS-UPDRS
		Mean (SD)	Mean (SD)	Mean (SD)	Mean (SD)	Controls	Cases	Mean (SD)	Mean (SD)	Mean (SD)	Mean (SD)			
Tao Wu	Tao Wu	63.7 (5.1)	64.0 (4.0)	38	57	59.2 (3.0)	4.8 (3.9)	16	14	Not available				
UCSF	UCSF	66.0 (6.3)	63.4 (7.5)	31	38	NA	NA	16	24	Yes				
Udall	Udall	62.5 (10.0)	64.9 (9.3)	61	30	NA	8.6 (5.0)	18	23	Not available				
Campinas	UNICAMP	60.0 (8.4)	60.2 (10.2)	62	31	52.6 (12.0)	7.6 (6.6)	120	97	Yes				
UPenn	UPenn	65.2 (6.4)	70.0 (7.2)	63	33	60.3 (8.3)	9.2 (5.9)	27	49	Yes				
Total		59.9 (11.8)	63.2 (9.7)	48	38	58.0 (10.5)	5.4 (5.1)	1212	2487					

Abbreviations: SD, standard deviation; MDS-UPDRS, Movement Disorder Society sponsored revision of the Unified Parkinson's Disease Rating Scale.

*Data only available for a subset of cases.

**Data missing for 1 patient

Statistical Analysis

All statistical analyses of cerebellar volume were carried out using R version 4.1.0.³¹ We fit linear mixed effects regression models (LMM) using lme4 and lmerTest packages in R, with diagnosis (ie, control or PD), age, sex, and ICV as fixed factors and cohort as a random intercept. The main analysis investigated differences in total cerebellar volume (sum of all 28 cerebellar regions of interest [ROI]) and each cerebellar lobule individually, in all people with PD versus controls, using model 1:

$$\text{Volume} \sim \text{Diagnosis} + \text{Age} + \text{Sex} + \text{ICV} + 1 \mid \text{cohort.} \tag{1}$$

ICV was included to control for between-subject differences in head size, which explains a substantial proportion of inter-individual variability (of non-interest) in brain volumetric assessments. In addition to modeling cohort as a random intercept in our linear mixed models, we also ran COMBAT on our raw dataset to correct for site-related heterogeneity. Results and comparisons of the results from the linear mixed models for COMBAT-corrected data and model 1 are reported in the Supporting Data. For HY stage-specific analyses, we selected a subsample of controls matched on age and sex to each HY stage. To do this, we used the nearest neighbor-matching procedure implemented in the MatchIt package for R,³² to select an age- and sex-matched subsample of controls for each HY group based on a propensity score estimated with logistic regression (MatchIt “glm” distance measure, ratio 2, caliper 0.15). Using this approach ensured that HY stages could be qualitatively compared. Matched subsamples were assessed using a two-sample Kolmogorov–Smirnov test for age and the χ^2 test for sex. Model 1 was repeated for each of the HY stage-specific analyses. For all analyses, results were false discovery rate (FDR) ($P < 0.05$) corrected for multiple comparisons. Cohen's *d* effect sizes with 95% confidence intervals were calculated for each of the ROIs, based on the estimated marginal means and Satterthwaite's approximation for degrees of freedom.³³ Negative effect size values correspond to people with PD having lower values relative to controls.

We used linear mixed effects models to test for associations between each ROI volume (and total cerebellar volume) and (1) motor symptom severity (MDS-UPDRS3 total score) and (2) time since diagnosis. For these models, age, sex, and ICV were modeled as fixed factors, and cohort as a random factor. For assessment with motor symptom severity, our primary analysis focused on MDS-UPDRS3 scores that were measured during the person's “OFF” state. If both ON and OFF state scores were available for each individual with PD

TABLE 2 Demographic and clinical characteristics of the HY samples

HY stage	n	Age, years (SD)	Sex, % female	Age at onset (SD)	Time since Diagnosis, y	MoCA score (SD)	MDS-UPDRS3 (SD)
HY1	354	58.7 (9.1)	43	56.2 (10.2)	2.5 (2.8)	27.2 (2.5)	OFF state: 16.1 (8.7) ON state: 16.0 (7.3)
HY2	1252	63.2 (9.1)	37	58.8 (10.0)	4.5 (4.5)	26.3 (3.0)	OFF state: 29.9 (11.6) ON state: 30.0 (14.6)
HY3	291	65.8 (9.7)	43	57.2 (12.3)	8.6 (6.4)	23.9 (4.0)	OFF state: 39.0 (13.9) ON state: 40.3 (16.0)
HY4–5	86	67.0 (10.1)	45	54.0 (11.8)	13.0 (6.2)	20.1 (5.0)	OFF state: 56.3 (12.8) ON state: 55.4 (18.8)

Note: HY stage information not available for all people with Parkinson's disease.

Abbreviation, HY, Hoehn and Yahr; MDS-UPDRS3, Movement Disorder Society sponsored revision of the Unified Parkinson's Disease Rating Scale part 3; MoCA, Montreal Cognitive Assessment; SD, standard deviation.

($n = 1$ cohort), the OFF state score was selected and used as a fixed factor in the model. Here, "OFF" state is when the research team determines the participant is not receiving benefit from dopaminergic treatment, such as after a scheduled stop in therapy before the research session.²⁷ For these analyses, partial η^2 is reported as a measure of effect size. Finally, to assess the relationship between cerebellar volume and cognitive ability within the entire sample, we first fit a linear mixed model with MoCA score, age, sex, MDS-UPDRS3 score, and ICV modeled as fixed factors, and cohort as a random factor. MDS-UPDRS3 score was included in the model because we wanted to test for the association between cerebellar volume and cognition independent of disease progression. Next, we stratified the PD group based on their MoCA scores, into cognitively impaired (MoCA score <26) and cognitively normal (MoCA score ≥ 26) groups and fit the above linear model to test for differences in regional and total cerebellar volume.³⁴

Results

Complete Sample

Demographics

A two sample t test showed that, on average, the people with PD were significantly older than the controls (mean age for people with PD, 63.2; SD, 9.7; mean age controls, 59.9; SD, 11.8; [$t_{3697} = -8.9$], $P < 0.001$). There were significantly more males in the PD group (62%) compared to controls (52%), $\chi^2(1, n = 3698) = 37.6$, $P < 0.001$.

Total and Regional Cerebellum Volume

There were no significant between-group differences in total (gray and white) cerebellar volume in people with PD versus controls ($P > 0.05$ FDR). ROI analyses,

however, revealed significantly lower gray matter volume in people with PD in three cerebellar lobules with small effect sizes ($d_{\min} = -0.11$, $d_{\max} = -0.15$, all $P < 0.05$ FDR) (Figure 1). Effects were localized to the superior posterior lobe, specifically left and right VIIB and right Crus II. There were no significant between-group differences for the remaining cerebellar lobules (Supplementary Table S3). An additional sensitivity analysis with an age and sex-matched subsample of 1195 people with PD (49% female; mean age, 60.2; SD, 9.8) and 1195 controls (51% female; mean age, 61.0; SD, 10.5) revealed lower volume of left and right VIIB and right Crus II in PD, with similar effect sizes (see Supplementary Table S4).

Associations with Time since Diagnosis, Motor Symptom Severity, and MoCA Scores

A total of 2297 people with PD had time since diagnosis scores available for analysis and 1189 had MDS-UPDRS3 scores obtained in the OFF state. There was no significant association between time since diagnosis and total or regional cerebellar volume, in PD participants (all $P_{\text{FDR}} > 0.05$). There were no significant associations between overall motor symptom severity and total or regional cerebellar volume. A trend negative relationship between motor symptom severity and total cerebellar volume was observed ($P_{\text{FDR}} = 0.06$). Given the known role of the cerebellar motor lobe (particularly lobules IV and V) in resting tremor in PD,^{23,35} we examined associations between left and right lobule V volume and total left and right tremor MDS-UPDRS3 subscale scores. In addition, associations with rigidity and bradykinesia subscale scores were assessed. Methodological details can be found in the Supporting Data. Results showed a significant negative correlation between right limb tremor and right cerebellar lobule V volume in the full sample ($P = 0.02$). In HY1

($n = 148$), there was a significant positive correlation between left limb rigidity ($P = 0.02$) and right limb rigidity ($P = 0.03$) and right lobule V volume.

In the total PD sample, 1252 individuals had MoCA and MDS-UPDRS3 scores available for analysis. There was a significant positive association between total cerebellar volume and MoCA score, independent of time since diagnosis in people with PD ($P_{FDR} = 0.002$). Compared to cognitively normal people with PD ($n = 846$), cognitively impaired people with PD ($n = 473$) showed significantly lower total cerebellar volume ($d = -0.17$, 95% $[-0.02, -0.30]$; $P = 0.01$). Post hoc analyses showed that this finding remained significant after adjusting for motor symptom severity and time since diagnosis.

HY Stage Analyses

The matching procedure selected 689 controls to match the 345 HY1 participants, 1018 controls to match the 1018 HY2 participants, 557 controls to match the 281 HY3 participants, and 164 controls to match the 82 HY4–5 participants. The included controls partially overlapped across stage analyses. Two 1-way ANOVAs across the four HY stage groups revealed significantly longer time since diagnosis and lower MoCA scores with increasing HY stages (Table 2).

HY1 versus Controls

Compared to controls, HY1 participants did not show significant differences in total cerebellar volume ($P_{FDR} > 0.05$). ROI analyses, however, revealed HY1 participants showed a higher volume of left and right lobule V in the anterior lobe ($d = 0.23$, 95% $[0.10, 0.35]$) and $d = 0.28$, 95% $[0.13, 0.42]$, respectively; all $P_{FDR} < 0.05$) (Figure 2; Supplementary Table S5).

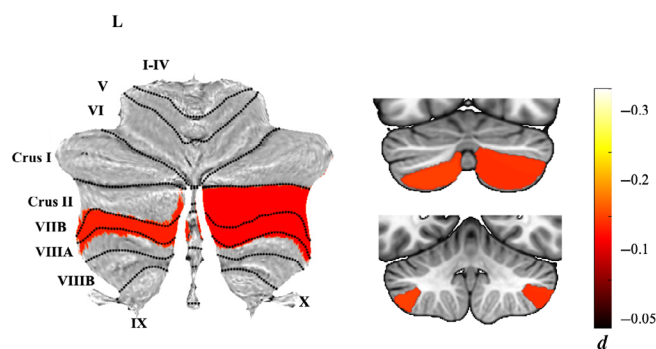


FIG. 1. Atlas-based effect size (Cohen's d) map, Montreal Neurological Institute (MNI)-based coronal slices (top: $y = -72$; bottom: $y = -54$) and forest plots (Cohen's $d \pm 95\%$ confidence interval) of the significant between-group differences for all people with Parkinson's disease (PD) versus controls. Negative effect sizes reflect people with PD $<$ controls. Regions significant at $P_{FDR \text{ corrected}} < 0.05$ are depicted in red. [Color figure can be viewed at wileyonlinelibrary.com]

HY2 versus Controls

HY2 participants did not show significant differences in total cerebellar volume or regional cerebellar volume, compared to controls ($P > 0.05$ FDR) (Supplementary Table S6).

HY3 versus Controls

Compared to controls, HY3 participants showed significantly lower total cerebellar volume ($d = -0.15$, 95% $[-0.02, -0.31]$). ROI analyses revealed lower gray matter volume of superior posterior lobe regions left and right lobule VIIIB ($d = -0.31$, 95% $[-0.12, -0.50]$) and $d = -0.35$, 95% $[-0.15, -0.53]$) and right Crus II ($d = -0.25$, 95% $[-0.09, -0.42]$); all $P_{FDR} < 0.05$ (Supplementary Table S7).

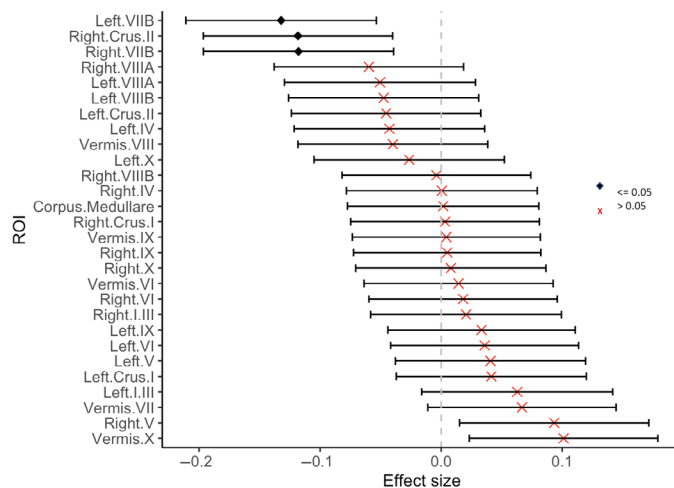
HY4–5 versus Controls

HY4–5 participants showed significantly reduced total cerebellar volume compared to controls ($d = -0.42$, 95% $[-0.09, -0.76]$). As in HY3, HY4–5 participants also showed a significantly lower volume of left and right lobule VIIIB compared to controls, but of a larger magnitude (left $d = -0.76$, 95% $[-0.44, -1.1]$) and right $d = -0.76$, 95% $[-0.42, -1.1]$); all $P_{FDR} < 0.05$. In addition, there was a significantly lower volume of the inferior posterior lobule left VIIIB ($d = -0.45$, 95% $[-0.13, -0.78]$) (Figure 3; Supplementary Table S8).

Post Hoc Analyses

HY Side-by-Side Comparison

Additional analyses comparing HY stages side-by-side showed significantly larger bilateral left and right lobule V in the HY1 group versus HY4–5 group



($P_{\text{FDR}} < 0.05$) (see Supplementary Figure S1). The left V lobule in HY1 was also significantly larger than in HY2 and HY3 groups ($P_{\text{FDR}} < 0.05$). Lobule VIIB was significantly smaller in the HY4–5 group bilaterally compared to HY1 and HY2 groups (all $P_{\text{FDR}} < 0.05$). The right VIIB lobule was also significantly smaller in the HY3 group compared to the HY1 group ($P_{\text{FDR}} < 0.05$).

Discussion

In the largest, most comprehensive assessment of regional cerebellar volume in PD to date, we show evidence of regionally specific alterations in anterior and posterior cerebellar lobe volume in PD associated with different clinical stages of the disease. Whereas less severe disease stages (HY1) were associated with larger anterior “motor” lobe regions, more severe disease stages (HY3, HY4–5) were associated with lower volumes principally weighted to posterior “non-motor” lobes of the cerebellum. Lobule VIIB showed a non-linear pattern of lower volume with each HY-increment bilaterally, with the most significant group differences in HY4–5 compared to controls. Total cerebellar volume was significantly lower in PD participants with cognitive impairment compared to cognitively normal PD, independent of motor symptom severity.

The spatial non-uniformity of cerebellar volume differences associated with disease staging suggests a targeted involvement of motor cerebellar pathways during the earlier course of the disease and non-motor cerebellar pathways in the later stages of the disease. Our finding of larger bilateral lobule V in HY1 is partially supported by previous work demonstrating higher anterior lobe volume in PD.²³ Although we found no significant relationship between MDS-UPDRS3 total score and lobule volume, we showed in a subset of the PD sample that alterations of anterior lobe volume in people with PD map onto specific motor symptoms of the disease. Specifically, greater total right limb tremor was associated with smaller right anterior lobule V volume, although this finding was not significant in the (much smaller) HY1 group. Our observations sit apart from previous structural and functional MRI studies that report a positive correlation between cerebellum anterior lobe volume and severity of total tremor,²³ as well as tremor-related activity and severity of rest tremor in PD.³⁶ Moreover, our findings are in line with a previous study showing a negative correlation between the cerebellum lobe VIIB and tremor severity in PD.³⁷ These contradicting observations are possibly explained by interindividual differences in the pathophysiology of tremor that determine the level of cerebellar influence.³⁸ The suggested opposite relationship between cerebellar volume and tremor versus rigidity may relate to the

known inverse relationship between rigidity and tremor symptoms in people with PD.³⁹ Collectively, our findings suggest that anterior lobe morphology is related to two core motor symptoms and supports the clinical relevance of these findings.

Higher anterior (motor) lobe volume in people with PD early in the disease course may be reflective of pre-morbidly larger anterior lobes, that retains their abnormal size in the early disease stage. It has been shown that genetic vulnerability to PD is associated with increased cortical surface area⁴⁰ and higher ICV⁴¹ and that people with PD, on average, have higher ICV compared to controls.¹ These findings are suggestive of a neurodevelopmental component (ie, brain overgrowth) underlying PD, which may explain selectively larger regions such as the cerebellum and thalamus. It is also possible that enlarged anterior lobes in PD are a consequence of hypermetabolic activity in response to dysregulated subcortical circuits of the basal ganglia.^{42,43} The anterior lobe of the cerebellum is preferentially connected to motor-related regions of the cerebral cortex, including the premotor and motor cortex, through feedforward (corticopontine projections) and feedback (cerebello-thalamo-cortical) closed loops. Until recently, the motor loops of the cerebellum and basal ganglia were thought to be anatomically separate and to perform distinct motor functions.⁴⁴ However, anatomical tracing studies in rats and monkeys have shown evidence for two disynaptic projections from the cerebellum to the striatum via the thalamus, and from the subthalamic nucleus (STN) to the cerebellum via the pontine nucleus, implying two-way communication between the cerebellum and basal ganglia.^{45,46} Temporary hypertrophy (eg, synaptogenesis) of the anterior lobe of the cerebellum could be driven by afferent and efferent cerebellar projections; first, abnormally high STN activity is thought to play a major role in the expression of motor features and leads to abnormal excitement of the cerebellar cortex.⁴⁷ Second, PD tremor specifically has been linked to basal ganglia-mediated hyperactivation of the cerebellothalamic pathway,^{36,48} and may be contingent on higher thalamic volume in early PD.¹ Critically, our findings suggest that higher anterior lobe volume in PD is not sustained over time and diminishes with progression of the disease.

In contrast to the anterior lobe, posterior lobe volume was significantly lower in the PD group relative to controls and showed incremental decreases with more severe disease staging. Lobule VIIB, which showed the largest differences across stages, is a “non-motor” region of the cerebellar cortex and is preferentially connected to prefrontal and posterior parietal regions of the cerebral cortex.^{13,49} Functional mapping studies ascribe this region to language and attentional processes.^{9,14} Functionally, this region is also part of the

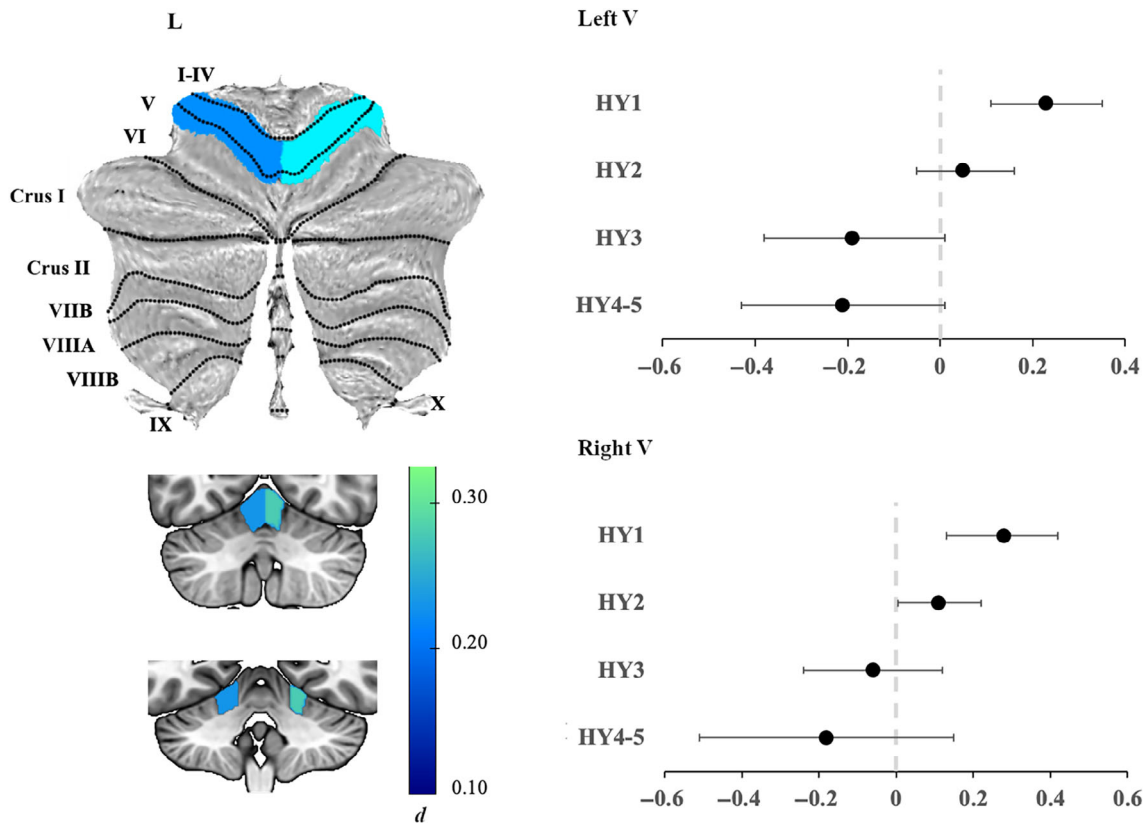


FIG. 2. (Left) Atlas-based effect size (Cohen's d) map and MNI-based coronal slices (top: $y = -62$; bottom: $y = -48$) of the significant between-group differences for Hoehn and Yahr (HY)1 participants versus controls. Regions significant at $P_{FDR\ corrected} < 0.05$ are depicted in blue. (Right) Effect sizes for left (top) and right (bottom) lobule V cerebellar volume associated with each disease stage. Negative values reflect lower volume in the Parkinson's disease group compared to controls. Bars represent 95% confidence intervals. [Color figure can be viewed at [wileyonlinelibrary.com](https://onlinelibrary.wiley.com)]

frontoparietal resting state network, which is selectively vulnerable to neurodegeneration and has been implicated in PD with and without associated cognitive decline.⁵⁰ Our findings align with an ongoing neurodegenerative process in the posterior lobe; each HY increment replicates the pattern of lower volume in bilateral VIIIB from the previous stage, denoted by larger group differences and further substantiated by statistically significant differences between disease stages. Notably, our findings were associated with the clinical state (disease stage), but not with time since diagnosis (disease duration). It remains unclear whether this cerebellar degeneration results from primary disease-related pathology or, if it is a secondary consequence of cortical and basal ganglia degeneration and associated progressive loss of functional capacity.

The association between worse cognitive performance and smaller cerebellar volume supports a growing body of empirical evidence for an instrumental role of the cerebellum in cognitive (non-motor) functioning in PD.^{16,51} Notably, this relation was not specific to any lobule, indicating a general relationship with cerebellar degeneration as the disease advances. Indeed, each increment of the HY stages was characterized by worse cognitive performance, motor performance, and longer

time since diagnosis. Future studies of functional connectivity changes of cerebellar lobules with the cerebral cortex across disease stages in PD and their associations with particular domains of cognition may yield insight into the functional reorganization of the cerebellum that occurs with disease progression and associated cognitive decline.

We found no associations with time since diagnosis, which seems counterintuitive in view of the progressive nature of PD. Of note, is that the time between disease onset, symptom presentation, and clinical diagnosis may differ substantially across individuals with PD, depending on sex and type of symptoms.^{52,53} Time since diagnosis may not, therefore, be a fully representative estimate of disease duration and severity. A recent meta-analysis of functional imaging studies in PD similarly found no significant relationship with time since diagnosis.⁵¹

Some limitations deserve attention. First, using cross-sectional data limits the strength of inferences we can make on disease progression and precludes our ability to track diagnostic accuracy over time. Although we cannot rule out the possibility that a small number of individuals with atypical forms of parkinsonism were included in our patient group, our large sample

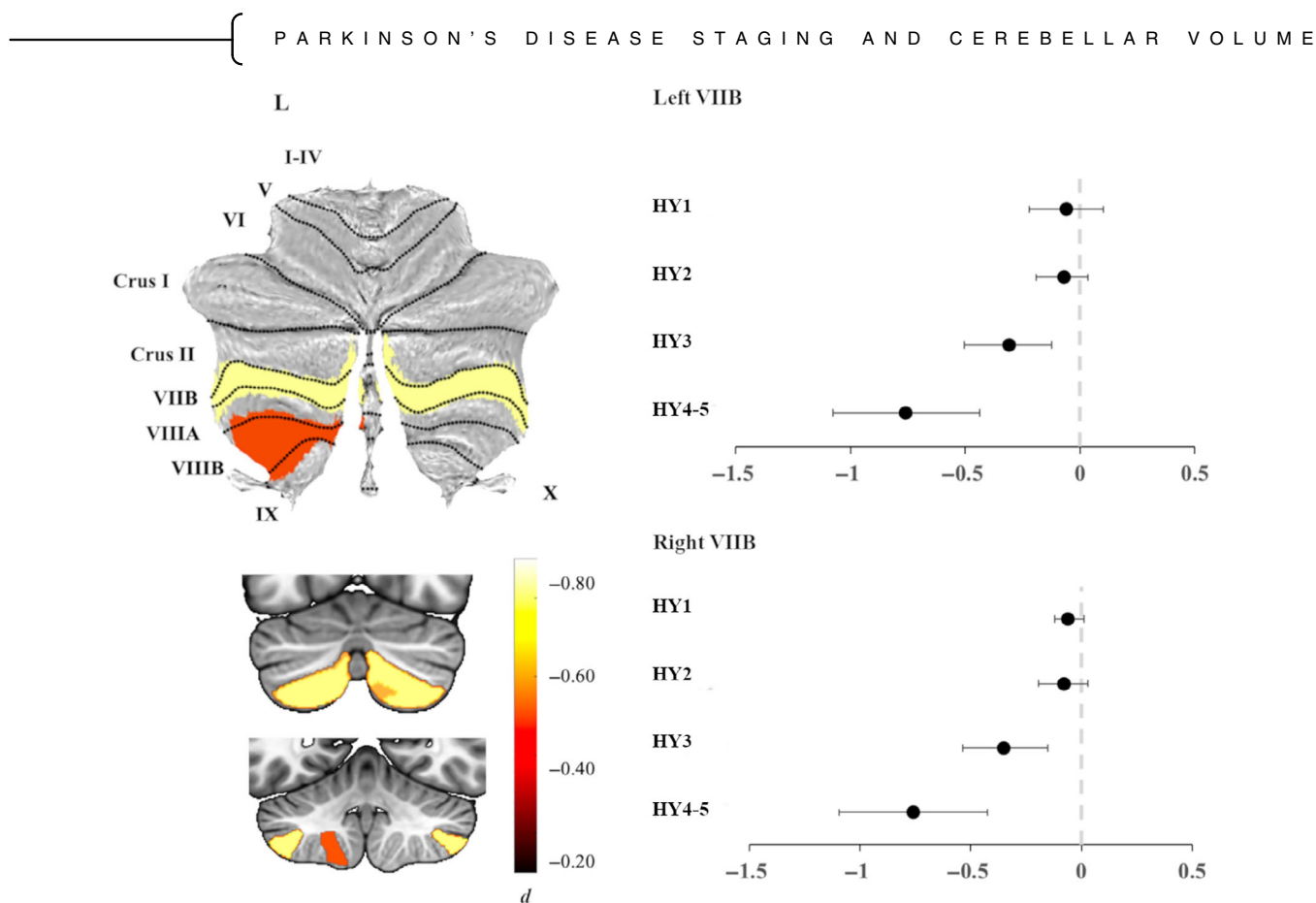


FIG. 3. (Left) Atlas-based effect size (Cohen's d) map and MNI-based coronal slices (top: $y = -72$; bottom: $y = -54$) of the significant between-group differences for Hoehn and Yahr (HY)4–5 participants versus controls. (Right) Effect sizes for left (top) and right (bottom) lobule VIIIB cerebellar volume associated with each disease stage. Negative values reflect lower volume in participants compared to controls. Bars represent 95% confidence intervals. [Color figure can be viewed at [wileyonlinelibrary.com](https://onlinelibrary.wiley.com)]

provides high confidence that the findings are representative of the PD population. Moreover, we show disease patterns that agree with expected ongoing degeneration and that largely replicate our previous findings.¹ Second, not all clinical measures were available for all cohorts, resulting in smaller samples for these analyses. Non-uniformity in the definition of OFF state for the MDS-UPDRS3 across sites confounds the interpretability of the results. Similarly, variability in the medication washout period between sites and across individuals may have influenced disease severity measures. The retrospective study design limits our ability to deeply investigate relationships between specific symptom domains and cerebellar structure, and control for the possible confounding of comorbidities (eg, alcohol abuse, nutritional deficiencies, and cerebrovascular disease). Third, whether the findings are PD-specific or overlap with related neurodegenerative diseases (eg, multiple system atrophy, progressive supranuclear palsy, and dementia with Lewy bodies) remains to be investigated.

In conclusion, we provide evidence of cerebellar structural alterations in PD, characterized by a dissociation between anterior and posterior cerebellar lobe

involvement that is associated with disease staging. Our results suggest that the changes in cerebellar volume are temporally ordered, with larger anterior “motor” lobe regions earlier in the course of the disease, and smaller posterior “non-motor” lobes in later stages. This study underscores the importance of incorporating the cerebellum into neurobiological models of PD. ●

Acknowledgments: We thank all the students and research assistants for their contribution to the data collection and analysis, in particular Lennart Zegerius and Liska Scheffers. We thank Sophia Thomopoulos for her continuous administrative support. In memoriam of Gianfranco Spalletta (August 8, 1962–March 18, 2023). Open access publishing facilitated by Monash University, as part of the Wiley - Monash University agreement via the Council of Australian University Librarians.

Data Availability Statement

Publicly available datasets used in this work include PPMI (ppmi-info.org), OpenNeuro Japan including Udall cohort (openneuro.org/datasets/ds000245/), and Neurocon and Tao Wu's data set (fcon_1000.projects.nitrc.org/indi/retro/parkinsons.html). The remaining cohorts are not all publicly available. Researchers are invited to register interest with the ENIGMA-PD Working Group to formally request data through secondary

research proposals. These proposals are considered by the working group leads and the individual site principal investigators. Any shared data are subject to individual data transfer agreements between each pair of participating institutions and investigators.

References

- Laansma MA, Bright JK, Al-Bachari S, et al. International multicenter analysis of brain structure across clinical stages of Parkinson's disease. *Mov Disord* 2021;36(11):2583–2594.
- Balsters JH, Ramnani N. Cerebellar plasticity and the automation of first-order rules. *J Neurosci* 2011;31(6):2305–2312.
- Buckner RL. The cerebellum and cognitive function: 25 years of insight from anatomy and neuroimaging. *Neuron* 2013;80(3):807–815.
- Ito M. Cerebellar circuitry as a neuronal machine. *Prog Neurobiol* 2006;78(3–5):272–303.
- Koziol LF, Budding D, Andreasen N, et al. Consensus paper: the cerebellum's role in movement and cognition. *Cerebellum* 2014;13(1):151–177.
- Baumann O, Borra RJ, Bower JM, et al. Consensus paper: the role of the cerebellum in perceptual processes. *Cerebellum* 2015;14(2):197–220.
- Schmahmann JD. The role of the cerebellum in cognition and emotion: personal reflections since 1982 on the dysmetria of thought hypothesis, and its historical evolution from theory to therapy. *Neuropsychol Rev* 2010;20(3):236–260.
- Shine JM, Shine R. Delegation to automaticity: the driving force for cognitive evolution? *Front Neurosci* 2014;8:1–8. <https://doi.org/10.3389/fnins.2014.00090>
- King M, Hernandez-Castillo CR, Poldrack RA, Ivry RB, Diedrichsen J. Functional boundaries in the human cerebellum revealed by a multi-domain task battery. *Nat Neurosci* 2019;22(8):1371–1378.
- Larsell O. The development of the cerebellum in man in relation to its comparative anatomy. *J Comp Neurol* 1947;87(2):85–129. <https://doi.org/10.1002/cne.900870203>
- Haines DE, Mihailoff GA. The cerebellum. *Fundamental Neuroscience for Basic and Clinical Applications*, 5th edition (Elsevier, Philadelphia, PA); 2018:394–412.e1. <https://doi.org/10.1016/b978-0-323-39632-5.00027-x>.
- Hoover JE, Strick PL. The organization of cerebellar and basal ganglia outputs to primary motor cortex as revealed by retrograde transneuronal transport of herpes simplex virus type 1. *J Neurosci* 1999;19(4):1446–1463.
- Kelly RM, Strick PL. Cerebellar loops with motor cortex and prefrontal cortex of a nonhuman primate. *J Neurosci* 2003;23(23):8432–8444.
- Buckner RL, Krienen FM, Castellanos A, Diaz JC, Yeo BTT. The organization of the human cerebellum estimated by intrinsic functional connectivity. *J Neurophysiol* 2011;106(5):2322–2345.
- Guell X, Gabrieli JDE, Schmahmann JD. Triple representation of language, working memory, social and emotion processing in the cerebellum: convergent evidence from task and seed-based resting-state fMRI analyses in a single large cohort. *Neuroimage* 2018;172:437–449.
- Gellersen HM, Guo CC, O'Callaghan C, Tan RH, Sami S, Hornberger M. Cerebellar atrophy in neurodegeneration—a meta-analysis. *J Neurol Neurosurg Psychiatry* 2017;88(9):780–788.
- Zeng LL, Xie L, Shen H, et al. Differentiating patients with Parkinson's disease from Normal controls using gray matter in the cerebellum. *Cerebellum* 2017;16(1):151–157.
- Piccinin CC, Campos LS, Guimarães RP, et al. Differential pattern of cerebellar atrophy in tremor-predominant and Akinetic/rigidity-predominant Parkinson's disease. *Cerebellum* 2017;16(3):623–628.
- O'Callaghan C, Hornberger M, Balsters JH, Halliday GM, Lewis SJG, Shine JM. Cerebellar atrophy in Parkinson's disease and its implication for network connectivity. *Brain* 2016;139(Pt 3):845–855.
- Chou KH, Lin WC, Lee PL, et al. Structural covariance networks of striatum subdivision in patients with Parkinson's disease. *Hum Brain Mapp* 2015;36(4):1567–1584.
- Nishio Y, Hirayama K, Takeda A, et al. Corticolimbic gray matter loss in Parkinson's disease without dementia. *Eur J Neurol* 2010;17(8):1090–1097.
- Pereira JB, Junqué C, Martí MJ, Ramirez-Ruiz B, Barrés-Faz D, Tolosa E. Structural brain correlates of verbal fluency in Parkinson's disease. *Neuroreport* 2009;20(8):741–744.
- Lopez AM, Trujillo P, Hernandez AB, et al. Structural correlates of the sensorimotor cerebellum in Parkinson's disease and essential tremor. *Mov Disord* 2020;35(7):1181–1188.
- Carass A, Cuzzocreo JL, Han S, et al. Comparing fully automated state-of-the-art cerebellum parcellation from magnetic resonance images. *Neuroimage* 2018;183:150–172.
- Han S, Carass A, He Y, Prince JL. Automatic cerebellum anatomical parcellation using U-net with locally constrained optimization. *Neuroimage* 2020;218:116819. <https://doi.org/10.1016/j.neuroimage.2020.116819>
- Kerestes R, Han S, Balachander S, et al. A standardized pipeline for examining human cerebellar Grey matter morphometry using structural magnetic resonance imaging. *J Vis Exp* 2022;180:1–26. <https://doi.org/10.3791/63340>
- Goetz CG, Tilley BC, Shaftman SR, et al. Movement Disorder Society-sponsored revision of the unified Parkinson's disease rating scale (MDS-UPDRS): scale presentation and clinimetric testing results. *Mov Disord* 2008;23(15):2129–2170.
- Nasreddine ZS, Phillips NA, Bédirian V, et al. The Montreal cognitive assessment, MoCA: a brief screening tool for mild cognitive impairment. *J Am Geriatr Soc* 2005;53(4):695–699.
- Goetz CG, Poewe W, Rascol O, et al. Movement Disorder Society task force report on the Hoehn and Yahr staging scale: status and recommendations. *Mov Disord* 2004;19(9):1020–1028.
- Goetz CG, Stebbins GT, Tilley BC. Calibration of unified Parkinson's disease rating scale scores to Movement Disorder Society-unified Parkinson's disease rating scale scores. *Mov Disord* 2012;27(10):1239–1242.
- R Core Team (2022). R: A language and environment for statistical computing. R Foundation for Statistical Computing, Vienna, Austria. URL <https://www.R-project.org/>
- Ho DE, Imai K, King G, Stuart EA. MatchIt: Nonparametric preprocessing for parametric causal inference. *J Stat Softw* 2011;42(8):1. <https://doi.org/10.18637/jss.v042.i08>
- Satterthwaite FE. An approximate distribution of estimates of variance components. *Biometrics* 1946;2(6):110–114.
- Dalrymple-Alford JC, MacAskill MR, Nakas CT, et al. The MoCA: well-suited screen for cognitive impairment in Parkinson disease. *Neurology* 2010;75(19):1717–1725.
- van den Berg KRE, Helmich RC. The role of the cerebellum in tremor – evidence from neuroimaging. *Tremor Other Hyperkinet Mov* 2021;11:49.
- Helmich RC, Janssen MJR, Oyen WJG, Bloem BR, Toni I. Pallidal dysfunction drives a cerebellothalamic circuit into Parkinson tremor. *Ann Neurol* 2011;69(2):269–281.
- Sadeghi F, Pötter-Nerger M, Grimm K, Gerloff C, Schulz R, Zittel S. Smaller cerebellar lobule VIIb is associated with tremor severity in Parkinson's disease. *Cerebellum* 2023;20. <https://doi.org/10.1007/s12311-023-01532-6>
- Dirkx MF, Zach H, van Nuland A, Bloem BR, Toni I, Helmich RC. Cerebral differences between dopamine-resistant and dopamine-responsive Parkinson's tremor. *Brain* 2019;142(10):3144–3157.
- Winogrodzka A, Wagenaar RC, Bergmans P, et al. Rigidity decreases resting tremor intensity in Parkinson's disease: a [(123)I] beta-CIT SPECT study in early, nonmedicated patients. *Mov Disord* 2001;16(6):1033–1040.
- Grasby KL, Jahanshad N, Painter JN, et al. The genetic architecture of the human cerebral cortex. *Science* 2020;367(6484). <https://doi.org/10.1126/science.aay6690>

41. Adams HHH, Hibar DP, Chouraki V, et al. Novel genetic loci underlying human intracranial volume identified through genome-wide association. *Nat Neurosci* 2016;19(12):1569–1582.
42. Wu T, Hallett M. The cerebellum in Parkinson's disease. *Brain* 2013;136(Pt 3):696–709.
43. Ingham CA, Hood SH, Mijster MJ, Baldock RA, Arbuthnott GW. Plasticity of striatopallidal terminals following unilateral lesion of the dopaminergic nigrostriatal pathway: a morphological study. *Exp Brain Res* 1997;116(1):39–49.
44. Kemp JM, Powell TP. The connexions of the striatum and globus pallidus: synthesis and speculation. *Philos Trans R Soc Lond B Biol Sci* 1971;262(845):441–457.
45. Hoshi E, Tremblay L, Féger J, Carras PL, Strick PL. The cerebellum communicates with the basal ganglia. *Nat Neurosci* 2005;8(11):1491–1493.
46. Bostan AC, Dum RP, Strick PL. The basal ganglia communicate with the cerebellum. *Proc Natl Acad Sci U S A* 2010;107(18):8452–8456.
47. Bostan AC, Strick PL. The basal ganglia and the cerebellum: nodes in an integrated network. *Nat Rev Neurosci* 2018;19(6):338–350.
48. Guehl D, Pessiglione M, François C, et al. Tremor-related activity of neurons in the “motor” thalamus: changes in firing rate and pattern in the MPTP vervet model of parkinsonism. *Eur J Neurosci* 2003;17(11):2388–2400.
49. Schmahmann JD. An emerging concept. The cerebellar contribution to higher function. *Arch Neurol* 1991;48(11):1178–1187.
50. Cascone AD, Langella S, Sklerov M, Dayan E. Frontoparietal network resilience is associated with protection against cognitive decline in Parkinson's disease. *Commun Biol* 2021;4(1):1021.
51. Solstrand Dahlberg L, Lungu O, Doyon J. Cerebellar contribution to motor and non-motor functions in Parkinson's disease: a meta-analysis of fMRI findings. *Front Neurol* 2020;11:127.
52. Breen DP, Evans JR, Farrell K, Brayne C, Barker RA. Determinants of delayed diagnosis in Parkinson's disease. *J Neurol* 2013;260(8):1978–1981.
53. O'Sullivan SS, Williams DR, Gallagher DA, Massey LA, Silveira-Moriyama L, Lees AJ. Nonmotor symptoms as presenting complaints in Parkinson's disease: a clinicopathological study. *Mov Disord* 2008;23(1):101–106.

Supporting Data

Additional Supporting Information may be found in the online version of this article at the publisher's web-site.